Programación Matemática y Software (2020) 12 (3): 1-8. ISSN: 2007-3283

Study, suspend and optimization a spread of epidemic infections. The dynamic Monte Carlo approach

Cómo estudiar, suspender y optimizar la propagación de infecciones epidémicas. El método dinámico de Monte Carlo

Gennadiy Burlak

Centro de Investigación en Ingeniería y Ciencias Aplicadas,
Universidad Autónoma del Estado de Morelos
Av. Universidad 1001, Col. Chamilpa, C.P. 62210, Cuernavaca, Morelos, México
Correo-e: gburlak@uaem.mx

KEYWORDS:

optimization of a spread of epidemic infections; dynamic Monte Carlo, numeric simulations.

ABSTRACT

We study a dynamics of the epidemiological infection spreading at different values of the risk factor β (a control parameter) with the using of dynamic Monte Carlo approach (DMC). In our toy model, the infection transmits due to contacts of randomly moving individuals. We show that the behavior of recovereds critically depends on the β value. For sub-critical values $\beta < \beta_c$ ~0.6 , the number of infected cases asymptotically converges to zero, such that for a moderate risk factor the infection may disappear with time. Our simulations shown that over time, the properties of such a system asymptotically become close to the critical transition in 2D percolation system. We also analyzed an extended system, which includes two additional parameters: the limits of taking on/ off quarantine state. It is found that the early quarantine off does result in the irregular (with positive Lyapunov exponent) oscillatory dynamics of infection. If the lower limit of the quarantine off is small enough, the recovery dynamics acquirers a characteristic nonmonotonic shape with several damped peaks. The dynamics of infection spreading in case of the individuals with immunity is studied too.

PALABRAS CLAVE:

optimization; epidemic infections; dynamic Monte Carlo, numeric simulations.

RESUMEN

Estudiamos una dinámica de la propagación de la infección epidemiológica a diferentes valores del factor de riesgo β (un parámetro de control) con el uso del enfoque dinámico de Monte Carlo (DMC). En nuestro modelo de juguete, la infección se transmite debido a los contactos de individuos que se mueven al azar. Mostramos que el comportamiento de los individuos recuperados depende críticamente del valor de β. Para valores subcríticos $\beta < \beta_c$ ~ 0,6, el número de casos infectados converge asintóticamente a cero, de modo que para un factor de riesgo moderado la infección puede desaparecer con el tiempo. Nuestras simulaciones mostraron que, con el tiempo, las propiedades de dicho sistema se acercan asintóticamente a la transición crítica en el sistema de percolación 2D. También analizamos un sistema extendido, que incluye dos parámetros adicionales: los límites de activación / desactivación del estado de cuarentena. Se encuentra que la cuarentena temprana da como resultado la dinámica oscilatoria irregular (con exponente de Lyapunov positivo) de la infección. Si el límite inferior de la cuarentena es lo suficientemente pequeño, la dinámica de recuperación adquiere una forma característica no monótona con varios picos amortiguados. También se estudia la dinámica de la propagación de la infección en el caso de los individuos con inmunidad.

Recibido: 08 de julio de 2020 • Aceptado: 01 de agosto de 2020 • Publicado en línea: 30 de octubre de 2020

1. INTRODUCTION

The dangerous dynamics of the coronavirus spread throughout the world gives rise to numerous studies in a wide scientific spectrum. Improving known epidemic models and developing new models are complicated tasks because the lack of verified statistics on the infection spread and disease dynamics. Unstable predictability of infection, ambiguity with drugs [1], uncertainty regarding the immunity of disease [2], and other factors (such as a viral mutation) make it difficult to predict the dynamics of pandemic. This may relay to some mathematical models, which depend on a significant number of free (statistically-driven) parameters. The known models of the SIR family give solutions in a form of smooth functions [3] (solutions of differential equations) that only indirectly include important random factors. Naturally, that in such a situation, most statistically reliable forecasts are obtained by methods based on the direct application of the central limit theorem with a predicted error of $1/\sqrt{N}$, see [4] [5] [6] and references therein. In this paper, we propose the use of the dynamic Monte Carlo (DMC) method that self-consistently includes various dynamic random factors. Such a technique was previously used to study the processes associated with aggregation, viscous flow properties, the formation of biological structures, and allows to scale the associated geometric and dynamic quantities that characterize these phenomena [7] [8] [9]. In our study, as a control (free) parameter, we use the generalized risk factor β, which includes some of the factors mentioned above in an integral form. In our 2D toy model, the transmission of infection occurs due to contacts of randomly moving individuals, that determines the complex dynamics of the infection spread and various critical aspects of such a dynamics. The paper is organized as follows. In Section 2, we formulate our approach and examine the behavior of infected individuals (order parameter $A(t, \beta)$), which, as it turns out latter, critically depends on the value β. It also is discussed the similarity of the asymptotic behavior of the infection dynamics with the critical phase transition in a two-dimensional (2D) percolation system. In the next Section, we analyze the dynamic properties of the extended system, where we deal with two additional parameters which allow to on/off the quarantine state. The next Section, contains the study of dynamics of the infection spreading and the formation of immunity for infected individuals. The last Section summarizes our conclusions.

2. DYNAMIC MONTE CARLO SIMULATIONS

First we explain which the properties of dynamic Monte Carlo (DMC) approach we deal with. In order to study the infection dynamic in epidemiological system (that is far from equilibrium) the DMC method is used, that allows investigation both temporal and spatial properties by the numerical simulations. As a toy model, we choose a 2D $L \times L$ (where L is size) bounded system that contains a disordered population of N individuals. Following the classifications commonly known from SIR model [3] in our DMC model we divide the host population into a set of distinct categories, according to its epidemiological status, that are susceptible (S), currently infectious (I), and recovered (R). The total size of the host population is then $N=S+I+R$ and all the individuals are born in the susceptible category [3]. Following the actual situations we assume that initially the maternally derived immunity is clear. (The effect of immunity is studied in the following sections).

Upon contact with infectious individuals, the susceptibles may get infected and move into the infectious category. To apply the DMC approach it is constructed the Person class (individual, alias object) that encapsulates properties of a randomly placed and moving individual and contains the following significant attributes

$$\{x, y, v_x, v_y, I, M\}, \tag{1}$$

where x, y are the components of position v_x, v_y are the components of velocity, the parameters I, M describe the states: infected/uninfected and immunized/non-immunized, respectively. The list of Persons that represents a total host population is used in our DMC simulations.

One of the underlying reasons why epidemiological systems exhibit variation is due to a different way that the individuals in a population have contact with each other. In our DMC simulation we assume that the spreading (transmission) of the infection occurs because of random contacts for moving individuals.

To do that in DMC simulations we use the following strategy. (i) Any contact can occur only between two nearest individuals. (ii) At any contact, the state of an infected transmits to the other contact person. But the infected one can still be recovered with probability $1\text{-}\beta$ (recall that $\beta \in [0, 1]$ is a risk factor). This means that if $\beta \lesssim 1$, the probability to a recovery is small.

To take an advantage of the visualizations at applying the DMC technique, we allow each object to have a visual representation, which is a yellow circle (non-immunized individual), a green circle (immunized but not infected individual) and a red circle (infected individual), see Figure 1. We used the interaction radius r as the unit scale to measure distances (used r=6, see Figure 1) between the individuals, while the time unit $\Delta t=1$ was the time interval between two updatings of the directions and positions. In our simulations we used the simplest initial conditions: at time $t=0$ the positions and velocities for all the N individuals are randomly distributed. We use the velocity scale such that random v_x, $v_y \in$ [2, 10] for which the individuals always interact with their actual neighbors and move fast enough to change the configuration after a few updates. According to our simulations, the variation of actual interval of values of v_x, v_y does not affect the results. We also investigated the cases when the basic parameter of the model, the density $\rho=N/L^2$ is slightly varied.

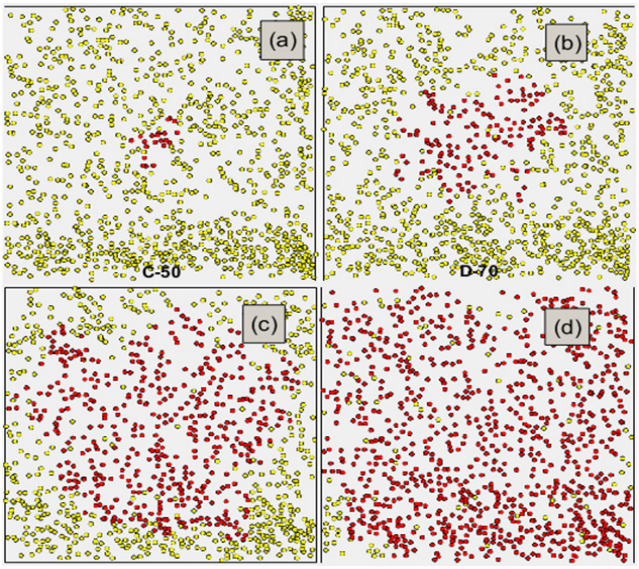

Figure 1 (Color online.) The snapshots (N = 1000; β = 0.95, L = 400) show the dynamics of the infection spreading at: (a) t=10, (b) t=30, (c) t=50, (d) t=70. We observe that for shown case at t = 70 nearly all the individuals are infected.

When the simulation time runs a lot contacts occur between nearest randomly moving persons that leads to fast and uncontrollable transfer of infection between many individuals, see Figure 1. It is of great interest to investigate the temporal infection dynamics at various risk factors β. Such a dynamics of the infections spreading (coefficient $A(t)=I(t)/(N)$) as function of time t is displayed in Figure 2. Since $A(t)$ is a random-valued function we will fit (see [10]) A(t) by a suitable fitting function that is chosen as

$$f(t) = a_0 t^{a_1} \tanh(t^{a_2}), \qquad (2)$$

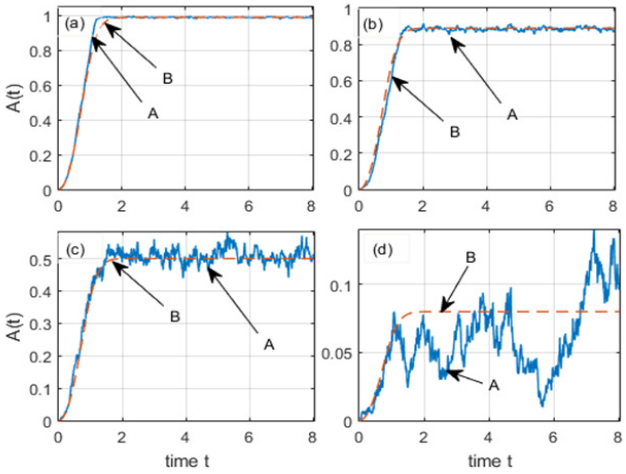

Figure 2 (Color on line.) The dynamics of the infections spreading coefficient (order parameter) $A=I/N$ for times $t<8$ at different values of the risk factor (control parameter) β. [In this figure the abscissa axis shows the fitting time 0.01t] The blue lines (arrows A) show the numerical simulations (DMC) data, while red lines (arrows B) display the fitting function Equation (2), where only a_0 coefficient changes considerably at β variation: (a) shows case β=0.99, (b) β= 0.90, (c) β= 0.80, (d) β= 0.60. At β < 0.60 the DMC solution rapidly converges to 0 (A = 0). This means that for $\beta < \beta c \approx 0.60$ all the infected individuals will be recovered up to t=8.

where $a_{0,\,1,\,2}$ are the fitting coefficients. We found that a_1 is very small $\sim 10^{-5}$ and $a_2 \simeq 2$ for all the cases, but the amplitude a_0 changes considerably at the β variation. In Figure 2 the blue lines show the numerical simulations (DMC) data, while the red lines display the fitting function $f(t)$. Figure 2(a) shows the case β=0.99, (b) β= 0.90, (c) β= 0.80, (d) β= 0.60. We indicate a *remarkable* observation that for $\beta < 0.60$ the system asymptotically converges to a trivial solution with $A \simeq a_0=0$ already for $t \simeq 6$. Such observation leads to an interesting assumption that the studied dynamics of the infection spread can (asymptotically) be associated with a critical transition in the two-dimensional (2D) percolation system, that

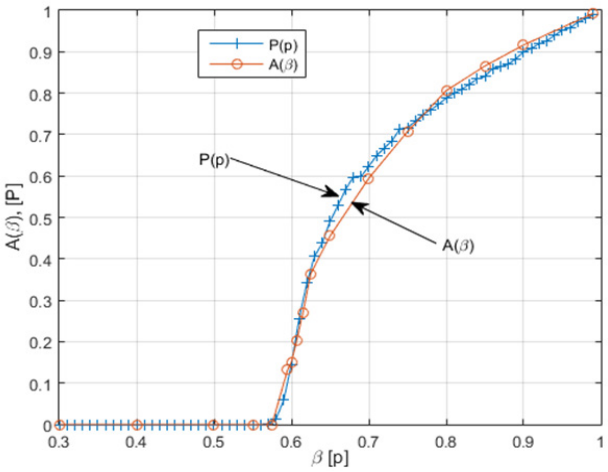

Figure 3 (Color online.) The comparison of the order parameter functions for the infection spreading $A(\beta)$ and the order parameter for 2D percolating $P(p)$, where p is the occupation probability of defect state [11]. Red line shows the dependence of (slightly tailored) amplitude parameter the fitting function a_0 corresponding to $A=I/N$ at fixed time $t=8$ as function of the risk factor β. Blue line shows the dependence of the order parameters $P(p)$ for 2D percolating material as function of the occupation probability p. We observe that both curves are very close and the phase transitions to infected/percolating state occurs similarly at $\beta_c \simeq p_c \simeq 0.6$ for both cases when the occupation probability of defects is $p_c=0.594$ [11], [12], [13], [14], [15] see Figure 3. Such an assumption is studied in the following Section.

3. CRITICAL VALUE OF THE RISK FACTOR

Figure 3 displays a comparison of above mentioned dependencies. In Figure 3 the red line shows the dependence $a_0(\beta)$ (see Figure 2) associated with the infecting parameter $A(\beta)=I/N$, and the blue line shows the percolating order parameters $P(p)$ as function of the occupation defect probability p. We observe that both dependencies are in excellent agreement and at $\beta_c \simeq p_c \simeq$ 0.6 the phase transition to infected/percolating state occurs. From Figure 3 we can assume that the parameter $A(\beta)$ can be mentioned further as an order parameter (similarly $P(p)$). This results that the formalism of the percolation critical percolating phase transition [11], [12], [13]can be applied to investigation the asymptotic of infection spreading at various (β). On the other hand, good agreement between the results of DMC modeling and the critical transition in 2D percolation system shows the general applicability of DMC approach to analyze the dynamics of infection spread in the epidemiological system.

4. THE EXTENSION OF MODEL

A. Quarantine regime

Mass infection shown in Figure 1 is an extremely dangerous and highly undesirable scenario for the development of epidemiological situation. This Section discusses the extension of the model, which in principle allows suspending this trend. One of the simple solutions proposed recently is introducing the quarantine by localizing of infected individuals in order to significantly reduce the number of contacts that leads to the transmission of infection. This can be modeled by setting $v_x=v_y=0$ for infected individuals and ignoring all the contacts with them in our approach. We call such a regime of simulation as a quarantine mode. In order to do this we introduce two new parameters into the model, A_{max} (the infection level when the quarantine is automatically turned on), and A_{min} (the infection level when the quarantine is turned off).

Figure 4 shows the dynamics of infections $A(t)$ in quarantine mode with A_{max}=0.7, A_{min}=0.36 at moderate values β, (a) β=0.78, (b) β=0.80, and (c) β=0.82; panel (d) shows the typical dynamics A at initial times. For such parameters from Figure 4 we observe that the system transmits to unexpected dynamic state: the generation of irregular oscillations of A with large amplitudes between A_{max} and A_{min}. We have calculated (by the method [16]) that the Lyapunov exponent for such irregular oscillations is about 0.3. This means that if quarantine is turned off too early, the growth of infections suppressed, but the system goes into dynamic mode with irregular oscillations. In this case, a significant number of infected and recovered individuals can be re-infected, therefore, a full recovery does not occur.

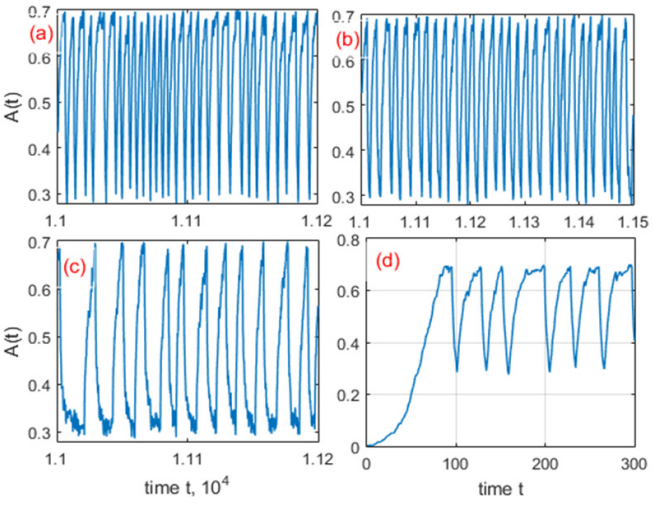

Figure 4 (Color online.) The dynamics of infection parameter A in quarantine mode with A_{max} = 0.7, A_{min} = 0.36 at moderate values, (a) β= 0.78, (b) β= 0.80, and (c) β=0.82; panel (d) shows the typical dynamics A at initial times. We observe the generation of irregular oscillations of A with large amplitudes between A_{max} and A_{min}. We calculated (by the method) that the Lyapunov exponent for such irregular oscillations is about 0.3.

Figure 5 shows the infections dynamics $A(t)$ in the quarantine mode but for large the risk factors β: (a) β= 0.88, (b) β= 0.90, (c) β=0.92, (d) β=0.88. We observe that for large β the evolution of the infections has monotonic shape (with small random variations) but without the oscillations as in Figure 4. However the dynamics $A(t)$ in (b) for β=0.90 is already suppressed and strongly differs with respect to a case without the quarantine shown in Figure 2(b).

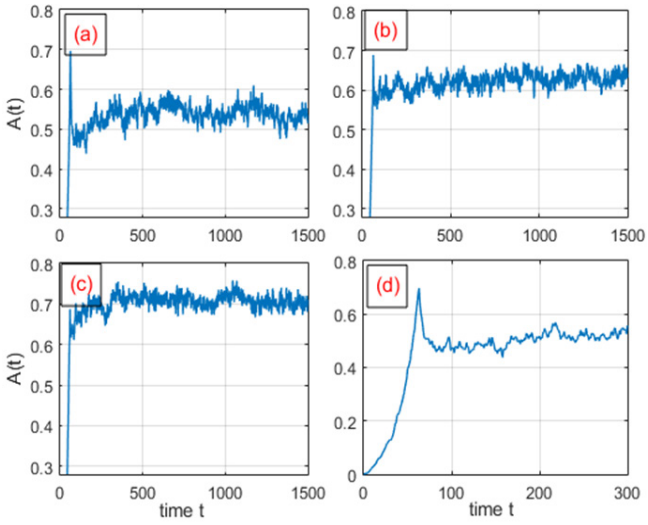

Figure 5 (Color online.) The same quarantine case as in Figure 4 but for large the risk factor β: (a) β=0.88, (b) β=0.90, (c) β=0.92, (d) β=0.88 for small times. We observe that for large the evolution of the infections has monotonic shape (with small random variations) but without the large oscillations shown in Figure 4. One can see that the dynamics $A(t)$ in (b) for β=0.90 is already suppressed and considerably differs with respect to situation without the quarantine shown in Figure 2(b).

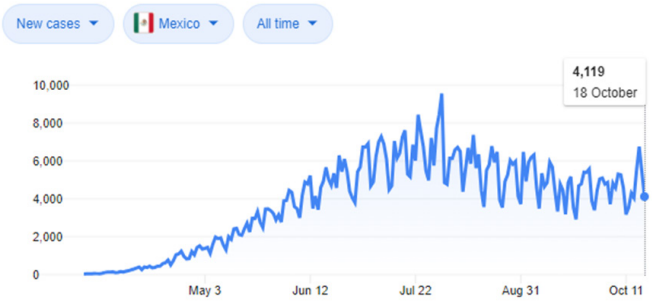

Figure 6. Current situation with COVID-19. We observe the irregular oscillating dynamics similar that is shown in Fig. 5.

B. The immunity

Although actually there are no reliable statistics for the congenital or acquired immunity for persons (for animals see Ref. [17]), in this Section we analyze this aspect in framework of our model. Following the Ref. [3], we assume that in the host population there is no innate immunity to the virus. But we suppose that the persons (at least a large majority) will acquire this immunity, as is usually the case. To this end, in our model we use the parameter M, see Equation (1). Following [3], we assume that this parameter acquires a non-zero value (the presence of immunity) only after first infection and recovery. Re-infection no longer occurs even at contacts with infected persons. Figure 7 shows the dynamics of recovery at presence of immunity in the quarantine mode for fixed parameters β=0.94 and A_{max}=0.24 and different A_{min}= 0.17, 0.1, 0.05, 0.02, 0.01. One can see that now the oscillations shown in Figure 6 acquire shape of strongly damped picks that results the number of infected (order parameter A) to rapidly decrease. This allows predicting that after the first high pick of infection (that has nearly fixed amplitude for all the cases) may occur a second pick but with lesser amplitude and then the complete recover may become.

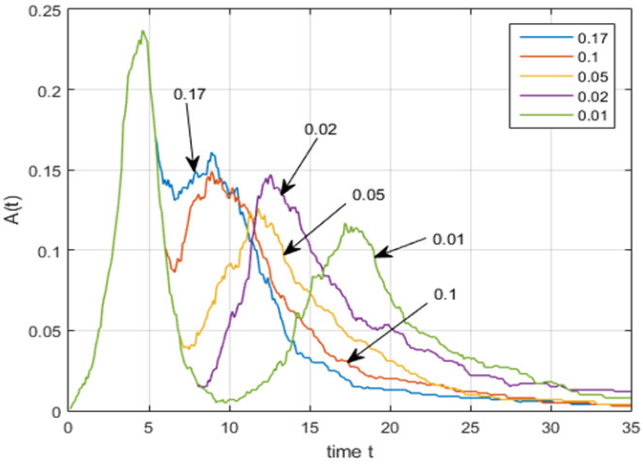

Figure 7 (Color online.) The dynamics of recovery in presence of immunity in the quarantine mode for the parameters β=0.94, A_{max}=0.24 for different A_{min}= 0.17, 0.1, 0.05, 0.02, 0.01. One can see that after the high peak, the oscillations rapidly decay that lead to a decrease of infections (the order parameter $A(t)$ rapidly decreases).

Now we compare the effects of quarantine and immunity factors for recovery. Figure 7 shows the dynamics of infections (order parameter A) for different values of the risk factor β=0.99, 0.94, 0.9, 0.8 at situation without the quarantine when only the personal immunity M>0 presents (see Equation (1)). This simulation shows that in such case the complete recover can occur even for a lesser time comparing to Figure 6.

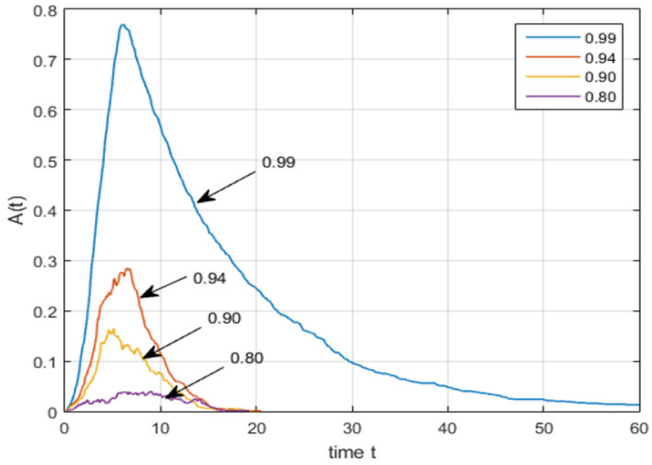

Figure 8 (Color online.) The dynamics of infections (order parameter A) for different values of the risk factor β=0.99, 0.94, 0.9, 0.8 for situation when only the effective personal immunity M > 0 presents (without the quarantine), see Equation (1). This simulation shows that in such case the complete recover can occur for a lesser time comparing to Figure 6.

5. DISCUSSION AND CONCLUSION

We studied the dynamics of the infection spread at various values of the risk factors β (control parameter) using the dynamic Monte Carlo method (DMC). In our model, it is accepted that the infection is transmitted through the contacts of randomly moving individuals. We show that the behavior of recovered individuals critically dependents on the value β. For sub-critical values β < βc ~0.6, the number of infected cases (the order parameters A(t) asymptotically converges to zero, so that at moderate risk factor, the infection can quickly disappear. However such a nontrivial behavior has to be confirmed by direct calculation.

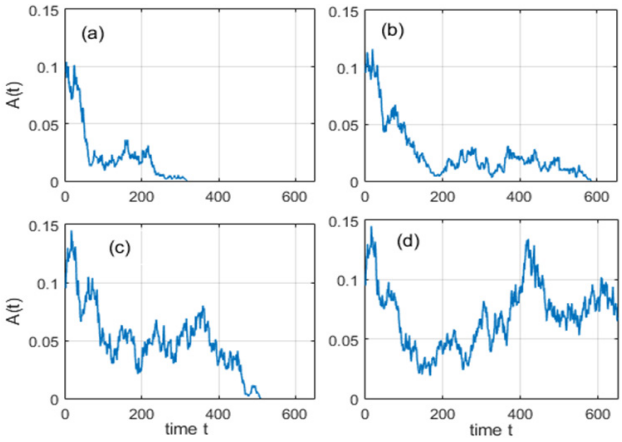

Figure 9 (Color online.) The fraction of infections $A(t, \beta)$ as function of time t at different risk factors near the critical transition at β_c ~ 0.6 for N=1000 and initial number of infections I_0=100, with β: (a) 0.56, (b) 0.57, (c) 0.58, (d) 0.581. We observe that for $\beta \lesssim 0.58$ the number of infections rapidly reaches zero. However for β>0.8 the process of recovering may be long.

Figure 8 shows the dynamics of infections fraction $A(t, \beta)$ with time for different risk factors β near the critical transition $\beta \sim \beta_c$ =0.6 for n=1000 and rather large the initial number of infections I_0=100. We observe that really for β ≲ 0.58 the number of infections rapidly reach zero. We also analyzed the extended system, which currently is widely used to prevent the spread of the virus. In our approach such a system includes two additional parameters on/off the quarantine state. It was revealed that early exit from the quarantine leads to irregular oscillating dynamics (with positive Lyapunov exponent) of the infection. However when the lower limit of the quarantine off is sufficiently small, the infection dynamics acquires a characteristic nonmonotonic shape with several damped peaks. The dynamics of the infection spread in case of individuals with immunity was studied too. Our comparison of quarantine and immunity during recovery shows that with stable immunity, complete recovery occurs faster than in quarantine mode. Finally, we apply the Monte Carlo approach to study the dynamics of the epidemic at different population number N, see Fig. 10, 11. We investigate the situations where all the individuals acquire stable immunity after illness and thus no longer capture an infection. This again confirms the importance of the personal immunity in a mass epidemic.

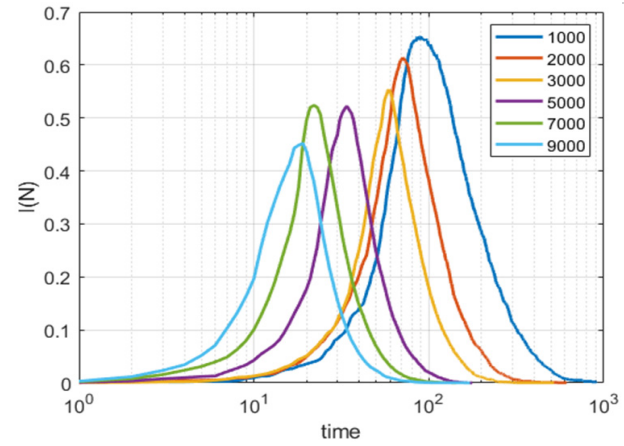

Figure 10. (Color on line.) The fraction of the infections I as function of time at different population number N=1000…9000 (size of the system is fixed L=400) at the risk factor β=0.98 for situation when the personal immunity $M > 0$ presents (without the quarantine). We observe that the larger N, the faster the recovery occurs, which again confirms the importance of the personal immunity in a mass epidemic.

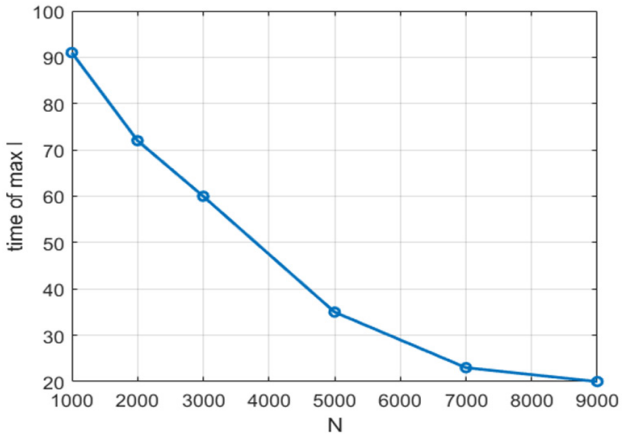

Figure 11. The time to reach the peak of infections I=I(N), depending on the population number N = 1000 ... 9000 (the size of the system is fixed L = 400) at the risk factor β=0.98 when the personal immunity $M > 0$ presents (without the quarantine). It can be seen that the larger the population N, the faster the peak of infection occurs, see Fig. 9. However, mass recovery with new acquired immunity is also faster.

From general point, it is instructively to compare the time behavior of the solutions of DMC and popular SIR model [3] for the same size of a host population N. The latter allows us to assure that the different DMC and SIR models can lead to similar results for S, I and R dependencies. To compare such dependencies which are calculated independently for DMC and SIR approaches we apply the Kolmogorov-Smirmov (K-S) statistics that is useful to verify the null hypothesis that both the data sets drawn from the same distribution, see details in Ref. [10]. From Fig.11 we observe a high similitude for S, I, R dependencies obtained independently from DMC simulations and numeric solution of SIR equations.

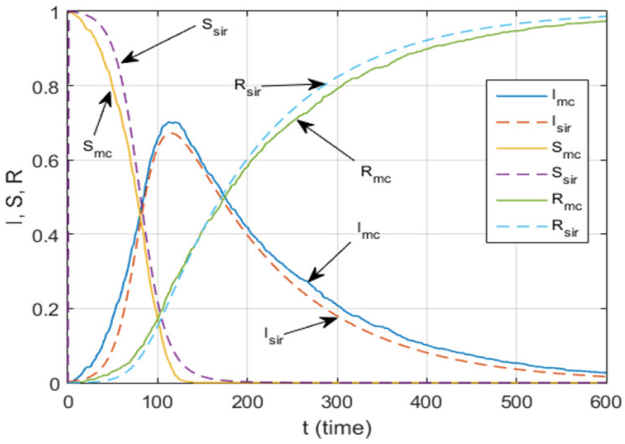

Figure 12 (Color on line.) Comparing DMC (solid lines) and SIR (dash lines) approaches for S; I and R dependencies. For SIR model all the functions are normalized by N value. For DMC approach are use parameter β=0.98. For SIR model is used a numerical solution of the SIR system. The factor 0.28 was used to adjust the time scales for the DMC and SIR models. We observe a high level of agreement for both DMC and SIR models for used parameters.

6. ACKNOWLEDGMENT

This work was supported in part by CONACYT (México) under the grant No. A-S-201.

REFERENCES

1. Corey, L., Mascola, J. R., Fauci, A. S., Collins, F. S. A strategic approach to COVID-19 vaccine R&D. Science. 20020, 368(6494), 948-950.
2. Coronavirus research updates: Potent human antibodies could inspire a vaccine, [En línea]. Available: https://www.nature.com/articles/d41586-020-00502-w.
3. Choisy, M., Guégan, J. F., Rohani, P. Mathematical modeling of infectious diseases dynamics. Encyclopedia of infectious diseases: modern methodologies, John Wiley & Sons, 2007, 379-404.
4. Barmparis, G. D., Tsironis, G. P.Estimating the infection horizon of COVID-19 in eight countries with a data-driven approach. Chaos, Solitons & Fractal. 2020, 135, 109842.
5. E. B. Postnikov. Estimation of COVID-19 dynamics "on a back-of-envelope": Does the simplest SIR model provide quantitative parameters and predictions?. Chaos, Solitons & Fractals, vol. 135, p. 109841, 2020.
6. Ndairou, F., Area, I., Nieto, J. J., Torres, D. F. Mathematical modeling of COVID-19 transmission dynamics with a case study of Wuhan. Chaos, Solitons & Fractals. 2020, 135, 109846.
7. Vicsek, T., Czirók, A., Ben-Jacob, E., Cohen, I., Shochet, O. Novel type of phase transition in a system of self-driven particles. Physical review letter. 1995, 75(6), 1226.
8. Solon, A. P., Chaté, H., Tailleur, J. From phase to microphase separation in flocking models: The essential role of nonequilibrium fluctuations. Physical review letters. 2015, 114(6), 068101.
9. Solon, A. P., Tailleur, J. Flocking with discrete symmetry: The two-dimensional active Ising model. Physical Review E. 2015, 92(4), 042119.
10. Press, W. H., Teukovsky, S. A., Vetterling, W. T., Flannery, B. P. Numerical recipes in C++. Cambridge: Cambridge University Press, 2002.
11. G. Grimmett. Percolation, second edition. Verlag: Springer, 1999.
12. M. B. Isichenko. Percolation, statistical topography, and transport in random media. Reviews of modern physics. 1992, 64(4), 961.
13. Stauffer, D., Aharony, A. Introduction to percolation theory. CRC press. 2018.
14. Burlak, G., Vlasova, M., Aguilar, P. M., Kakazey, M., Xixitla-Cheron, L. Optical percolation in ceramics assisted by porous clusters. Optics communications. 2009, 282(14), 2850-2856.
15. Burlak, G., Rubo, Y. G. Mirrorless lasing from light emitters in percolating clusters. Physical Review. 2015, 92(1), 013812.
16. Wolf, A., Swift, J. B., Swinney, H. L., Vastano, J. A. Determining Lyapunov exponents from a time series. Physica D: Nonlinear Phenomena. 1985, 16(3), 285-317.
17. Chandrashekar, A., Liu, J., Martinot, A. J., McMahan, K., Mercado, N. B., Peter, L., ... Busman-Sahay, K. SARS-CoV-2 infection protects against rechallenge in rhesus macaques. Science. 2020, 369, 812-817.

Acerca de los autores

Dr. Gennadiy Burlak, CIICAp de la UAEM.

El Dr. Gennadiy Burlak ha trabajado como catedrático en la Universidad Nacional de Kiev, en el Departamento de Física Teórica. Tiene los grados de doctor en: Ph. D. y D. of Sc. Desde 1998 es Profesor-Investigador Titular "C" del Centro de Investigaciones en Ingeniería y Ciencias Aplicadas (CIICAp) de la Universidad Autónoma del Estado de Morelos (UAEM). Es miembro del SNI desde 2000 y actualmente tiene el nivel III. El Dr. Burlak es autor y coautor de 14 libros y capítulos de libros y más de 160 artículos en revistas internacionales. Ha participado en más de 170 ponencias en Congresos Nacionales e Internacionales. Bajo de su dirección se han graduado: 16 tesis de doctorado, maestría y licenciatura. Ha impartido cursos de electromagnetismo, ecuaciones derivadas parciales y métodos numéricos en el posgrado y licenciatura del CIICAp de la UAEM. Es miembro de la Academia de Ciencias de Morelos (ACMOR) de American Physical Society. Se ha desempeñado como evaluador, árbitro del CONACyT y como referí de varias revistas internacionales como lo son: Phys.Rev.Lett., Chaos, JVSTA, MMA,PIER, entre otros. Sus temas principales de investigación son: - Micro-esféricas multicapas, -Optimización de radiación óptica en nanoestructuras, - Dinámica no-lineal del Bose-Einstein condénsate, - Aplicaciones de redes neuronales en física cuántica y transición de fases en sistemas sólidos.